Simulations of Ionic Liquids, Solutions, and Surfaces

RUTH M. LYNDEN-BELL,*,†,‡ MARIO G. DEL PÓPOLO,† TRISTAN G. A. YOUNGS,† JORGE KOHANOFF,† CHRISTOF G. HANKE,§ JASON B. HARPER,|| AND CARLOS C. PINILLA†

Atomistic Simulation Centre, School of Mathematics and Physics, Queen's University, Belfast BT7 1NN, United Kingdom, University Chemical Laboratory, Lensfield Road, Cambridge CB2 1EW, United Kingdom, Rechenzentrum Garching (RZG) Computing Centre, Max Planck Institute (MPI), Garching, Germany, and School of Chemistry, University of New South Wales, Sydney 2052, Australia

Received March 15, 2007

ABSTRACT

We have been using atomistic simulation for the last 10 years to study properties of imidazolium-based ionic liquids. Studies of dissolved molecules show the importance of electrostatic interactions in both aromatic and hydrogen-bonding solutes. However, the local structure strongly depends upon ion–ion and solute–solvent interactions. We find interesting local alignments of cations at the gas–liquid and solid–liquid interfaces, which give a potential drop through the surface. If the solid interface is charged, this charge is strongly screened over distances of a few nanometres and this screening decays on a fast time scale. We have studied the sensitivity of the liquid structure to force-field parameters and show that results from ab initio simulations can be used in the development of force fields.

1. Introduction

Liquids are difficult to model because the molecules are both in contact with each other (as in solids) and in perpetual motion (as in the gas phase). A proper description of a liquid must include the role of temperature and the consequent molecular motion. Thus, to model a liquid on a computer, one needs to follow the motion of the molecules over a time period; unlike a crystal, a single structure does not provide a sufficient description. The methods developed to do this are known as atomistic or molecular simulation, and two principal techniques, molecular dynamics and Monte Carlo, have been used for many years to study liquids and solutions.[1] These computational methods provide a succession of configurations of a liquid at some specified temperature and density or pressure from which one can find the average local structure as well as thermodynamic and dynamical properties. Because the modeling is molecular, one can determine the molecular basis of microscopic behavior and help to interpret experimental results. The Atomistic Simulation Centre at Queen's University Belfast pioneered the simulation of ionic liquids. The first empirical intermolecular potentials were developed by Sally Price in association with us and were used to study the structure and properties of neat dimethylimidazolium chloride, [dmim][Cl], in 2001.[2] This was shortly followed by other groups,[3–7] and now there is an increasing number of papers published using such simulation methods to investigate the behavior of room temperature ionic liquids.

Most of these simulations are classical as opposed to quantum mechanical. The interactions between molecules are modeled by empirical force fields rather than by solving the quantum mechanical problem of the electron energy. There is much experience in developing force fields for molecular liquids and solutions, which need to be a satisfactory compromise between accuracy and

* To whom correspondence should be addressed. E-mail: rmlb@cam.ac.uk.
† Queen's University.
‡ University Chemical Laboratory.
§ Max Planck Institute (MPI).
|| University of New South Wales.

Ruth Lynden-Bell received her Ph.D. degree from the University of Cambridge in 1962. She has been using atomistic simulation to study liquids, solutions, and other systems for many years. She moved to Queen's University from Cambridge in 1995 and returned to Cambridge as an emeritus professor in 2003, where she is still actively pursuing research in liquids and solutions.

Mario Del Pópolo received his Ph.D. degree in chemistry from the National University of Córdoba, Argentina, in 2002. After a year of postdoctoral work at the Henry Eyring Center for Theoretical Chemistry (University of Utah, Salt Lake City, UT), he joined the Atomistic Simulation Centre, at Queen's University Belfast, where he has held an academic position since 2006. His research interests focus on the statistical mechanics and computer simulation of condensed phase systems, with an emphasis on complex fluids and chemical reactivity.

Tristan Youngs received his Ph.D. degree from the University of Reading and has been working as a Research Fellow at Queen's University Belfast studying ionic liquids since 2004 and works closely with experimentalists to answer real-world questions that arise from this interesting class of solvents. He also has an interest in the investigation of model ionic liquids and the development of force fields to allow for more accurate simulations to be performed.

Jorge Kohanoff graduated from the University of Buenos Aires (Argentina) in 1986 and obtained a M.Phil. degree from SISSA (Italy) in 1990 and his Ph.D. degree from ETH Zurich in 1993, under the supervision of Michele Parrinello. Since 1990, he has been using and developing first-principle methods for calculating the properties of molecules and condensed phases. His main contributions are the area of semiconducting nanostructures (silicon and fullerenes), high pressure solids (hydrogen and sulphur) and fluids (plasmas), hydrogen-bonded crystals and liquids (KDP, ice, and water), and room temperature ionic liquids. He is a Reader at Queen's University Belfast, and in 2006, he published a textbook on Electronic Structure Calculations with Cambridge University Press.

Christof Hanke graduated 1999 with a diploma in physics in Wurzburg, Germany. He then obtained his Ph.D. degree at Queen's Unversity under the supervision of Prof. Lynden-Bell in simulation of ionic liquids. Upon graduation, he took a position at the RZG, the Computing Center of the Max-Planck-Society, in the area of data storage. Currently, he is a visiting expert at CSC, the Finnish IT center for science, as part of the DEISA project.

Jason Harper is a graduate of the University of Adelaide and the Australian National University and spent 2 years as a C. J. Martin Postdoctoral Fellow at the University Chemical Laboratory, Cambridge. Since 2002, he has held an academic position at the University of New South Wales, where his interests focus on rationalizing the outcomes of organic processes in ionic liquids. It was a visit to the Atomistic Simulation Centre in 2002–2003 that first showed him the use of molecular dynamics simulations in furthering this understanding.

Carlos Pinilla graduated in 2003 with a licentiate in physics from the Universidad Nacional of Colombia. He is currently a Ph.D. student at the Atomistic Simulation Centre, where he works on the simulation of complex ionic systems. He focuses on the study of dynamical and structural properties of confined ionic liquids. He also has an interest in investigating the response of these systems to external perturbations, as well as the use of ab initio methods to predict structural properties of their solid phase.

10.1021/ar700065s CCC: $37.00
Published on Web 10/04/2007

efficiency. Similar methods have been used to develop force fields for ionic liquids, and it has been proven possible to find force fields that are sufficiently accurate to describe the basic physics of the processes involved.

2. Finding and Improving Intermolecular Potentials

In a traditional simulation, the user supplies an intermolecular potential. Any such potential is bound to be an approximation to the interactions in a real liquid, and there is a trade-off between the accuracy of the potential and the computational cost of the calculation. In our group, we have used both our original potential[2] and various potentials proposed by other groups.[3,8] These potentials have mostly been developed from a combination of quantum chemical calculations on the isolated ions to find the charge distributions and standard intersite parameters describing the short-range repulsion and intermediate-range dispersion interactions. One expects that any potential that describes the essential physics of the interacting molecules should give a reasonable description of the liquid structure. However, to obtain the right dynamics requires a more accurate description of the intermolecular forces. Voth et al.[9,10] have investigated the effects of including polarizability in the potentials, which one imagines could be important in an ionic liquid. They find that the diffusion constant increases by a factor of 3 upon going from a nonpolarizable model to a polarizable one.

However, many years of experience with simulations of water have shown that reasonable descriptions of the liquid state can be obtained using nonpolarizable models but only if the dipole moment of the model molecule is increased over that calculated in the gas phase by a considerable amount. This takes into account the average polarization of the molecule in the liquid environment. We wondered whether there was a similar effect in the liquid phase of imidazolium ionic liquids and analysed the results of liquid state ab initio calculations to see whether there was a change in the dipole moment (or, equivalently, a shift in the center of the cation charge) in the liquid when compared to the gas phase. Figure 1 shows that there is an enhancement of both the average dipole moment and its fluctuations in the liquid. The change in the average dipole moment corresponds to a shift of the center of the charge by about 0.2 Å from the gas phase to the liquid and shows that even the average electrostatic properties of the ions are changed by the liquid environment.[11]

One way that we have explored the effects of the liquid environment and the construction of intermolecular potentials is to take the results from a quantum calculation and to find the best fit between the forces in an ab initio simulation[26] and those in a classical simulation when the intermolecular potential parameters are varied.[12] As well as allowing us to improve potentials for the simulation of these types of liquids, in some ways, this also provides a means to validate existing potentials derived by rather

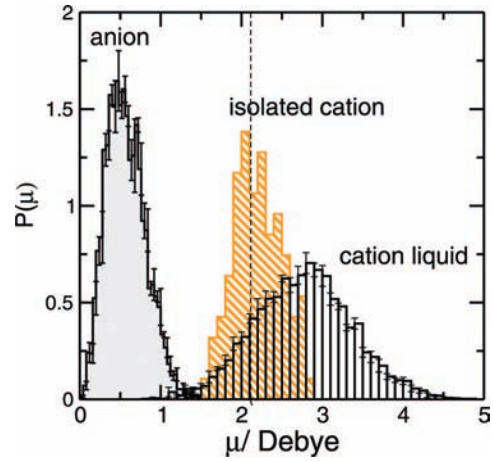

FIGURE 1. Distribution of instantaneous dipole moments for cations and anions in an ab initio calculation of [dmim][Cl]. This figure was reproduced from ref 11, copyright 2006, with permission from Taylor and Francis.

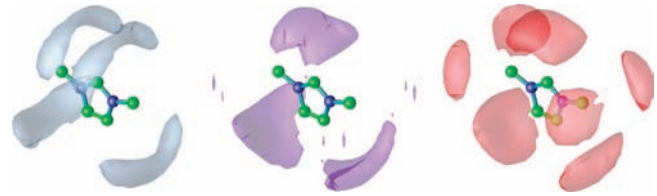

FIGURE 2. Probability distributions of chloride ions around a [dmim] cation calculated with Canongia Lopes' classical force field[8] (left), ab initio simulation[26] (middle), and Youngs classical force-matched potential[12] (right). The main differences are in the region of the unique CH, which points upwards. In Canongia Lopes' force field, the chloride ions tend to lie in bands on either side of this group, while in the ab initio simulation and the new force field, the chloride ions lie directly along the CH bond.

different methods. From the results of the fit, we observe a charge distribution similar to those calculated by molecular-electrostatic-potential-based methods applied to ions in the gas phase. In fact, if the charges of hydrogen atoms are summed into those of their respective heavy atoms, "coarse graining" the charge potential, the values are very similar to those of Canongia Lopes' model.[8] However, the three-dimensional distributions of ions in the liquid, which are shown in Figure 2, are quite different when calculated with these two models, with the fitted model more closely reproducing the ab initio calculated surfaces. Of course, this is also related to the different set of Lennard–Jones parameters used for the ions, for which the most significant changes occur for the hydrogen atoms, both on the imidazolium ring and in the attached methyl groups. Typically, both aliphatic and aromatic hydrogen atoms are assigned Lennard–Jones radii of around 2.5 Å in popular force fields, but the results of the fitting suggest that these may be rather generous for similar hydrogens in molten salt-like environments, offering radii approximately half this value. It can clearly be seen in radial distribution functions that all models in the literature reproduce, more or less, the general distribution of anions about cations, as seen in ab initio and neutron diffraction studies. However, the fine details of the interactions are often not adequately predicted.

Comparing ab initio calculated site–site radial distribution functions (RDFs) from hydrogen atoms of the cation to the anion, we observe that the classical peaks are at a noticeably longer distance and can display a simpler peak structure than the ab initio results. As a consequence of the smaller radii of the hydrogen atoms on the cation, these peak positions are shifted, so that they coincide with those observed in the ab initio curves. An unwanted side effect of the fitting is manifest as increased peak heights, but in general, the fitted model shows many improved features. Another problem is that the parameters in ref 12 do not give the correct density at 1 atm. One of the shortcomings of the density functional method used for the ab initio calculations is that long-range dispersion forces are not correctly described, and it is probably this shortcoming that is partly affecting the derived force field. Currently, Youngs is working on an improved model, but the current model does provide a good description of the local liquid structure at the experimental density.

From this optimized model, we have studied systematically the effect of modifying features of the force field and their effects on the properties of the liquid.[13] For instance, the local dipoles on the C–H bonds of the imidazolium ring were gradually reversed to study the structural consequences of removing the preferred interaction sites of the anion on the cation. This change is, of course, unphysical but shows how sensitive or otherwise the liquid properties are to the charge distribution. Once the direction of the imidazolium C–H dipoles has been reversed, the anion interaction with the cation proceeds primarily through the poorly coordinating methyl groups because these now provide the only accessible positively charged regions on the cation. Additionally, where cations once occupied the space directly above and below the plane of the imidazolium ring, once the imidazolium C–H dipoles have been reversed, these regions are populated by anions instead. Although anions in these positions above and below the rings have not previously been observed in simulations, they have been reported from the analysis of neutron diffraction experiments, raising interesting questions on one or both of these areas of study.

3. Dissolved Molecules

In view of the widespread use of ionic liquids as solvents, one of our particular interests was in the interactions with dissolved molecules and the local structure around them. Our experimental colleagues told us that, in general, protic solutes were more soluble than aprotic solutes, that aromatic solutes were more soluble than aliphatic solutes, and that they wondered why. Further, they hoped that an understanding of solvation might be used to understand the unusual reactivity of organic compounds in these solvents. Simulation is useful for investigating the reasons for general properties such as these, and in both cases, the answer turned out to be that it was electrostatic interactions that mattered.

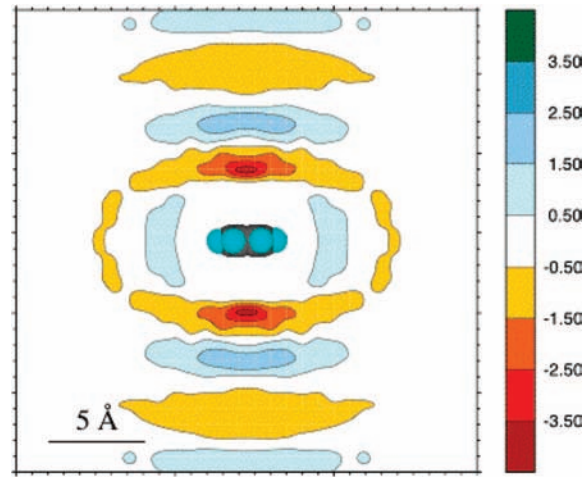

FIGURE 3. Difference of probability densities of cations and anions around a benzene molecule in [dmim][PF_6]. This is a sideways view of the cylindrically averaged distributions, with the benzene ring in the center. In the red regions above and below the plane of the benzene, there is a high probability of finding cations, while the anions favor the blue regions around the plane. This figure was reproduced from ref 14, copyright 2003, with permission from Elsevier.

FIGURE 4. Distribution of chloride ions (green) and sites on the [dmim] (blue and black) ions around a water molecule in [dmim][Cl]. Two chloride ions are hydrogen-bonded to the water OH groups and hold a cation between them. This figure was reproduced from ref 17, copyright 2002, with permission from The Royal Society of Chemistry.

If we consider benzene as an example of an aromatic molecule, we note that, although it has no dipole moment, it does have a significant quadrupole moment. The latter gives an electrostatic field, which attracts positive charges above and below the ring and negative charges around it. We found that the ions of the ionic liquid responded to these fields and formed a ring of anions around the equator of the molecule and that there was a high probability of finding cations above and below the benzene rings.[14,15] This is shown in Figure 3, which shows a cylindrical average of the difference between cation and anion probability densities around the ring of a benzene molecule dissolved in dimethylimidazolium hexaphosphate, [dmim][PF_6]. These distributions are in agreement with what would be expected from the electrostatic field. However, further analysis of the energetics of the interaction yielded a surprising result, namely, that the cations above and below the rings were not in the most favorable position relative to the rings but that their distribution was determined as much by the ion–ion interaction with

the anions forming the ring around the benzene ring as by the direct interaction with the electrostatic field of the benzene molecule itself. Similar studies with fluorinated benzene derivatives showed equivalent results, with inversion of the orientation in the case of hexafluorobenzene (which has a quadrupole moment of approximately the same magnitude but of opposite sign) and limited order in the case of 1,3,5-trifluorobenzene (which has a quadrupole moment of approximately zero).

Because aliphatic compounds have much smaller electrostatic fields than aromatic compounds, an uncharged version of benzene can be considered as a generic aliphatic compound. It is straightforward to calculate the change in free energy or chemical potential when a benzene molecule is transformed into an uncharged benzene molecule. This was found to be 22 kJ/mol in [dmim][Cl] and 12 kJ/mol in [dmim][PF_6], in both cases, a significant destabilization, which explains the observation that aliphatic compounds in general are less soluble than aromatic compounds.

The explanation of the greater solubility of protic than aprotic solutes also lies with the electrostatic interactions, in this case, the degree of hydrogen bonding of the solute with the anion. Simulation measurements[16] of the series of similar sized molecules found that the excess chemical potentials in [dmim][Cl] of the series water, methanol, and dimethyl ether are −29, −14, and +7 kJ/mol, respectively. This suggests that the addition of a hydrogen bond adds a stabilization of 15–20 kJ/mol. The additional stabilization is associated with changes in the local structure,[17] which are shown in Figure 4. This figure shows that the regions of high probability of finding chloride ions are along the OH bonds of the water molecule. Although one might have expected the region with the highest probability density of cations to be behind the water molecule, in fact, it is determined by ion–ion interactions rather than ion–water interactions and is in front of the water molecule between the chloride ions.

4. Gas–Liquid Interfaces

When an interface is formed, molecules near the interface feel fewer interactions and the free energy of a surface can often be reduced by local changes in the molecular orientation, density, or composition. Familiar examples include surface adsorption in solutions and the alignment of water molecules near the gas–liquid surface, so that the dipole moments lie in the surface.

The surfaces of ionic liquids show dramatic changes in the local structure, which can be demonstrated by simulation and probed by a number of experimental techniques. We have used simulation to investigate the surface structure in models of dimethylimidazolium [dmim][18,19] and butylmethyl imidazolium [C_4mim] ionic liquids with a number of inorganic anions.[20,21]

In the top layer of the surface, the cations are preferentially aligned with their rings perpendicular to the plane of the surface and their NN axes parallel to the surface normal. The dimethylimidazolium cation, [dmim], is symmetric, but the [C_4mim] cation shows a strong preference for the butyl group to point away from the bulk of the liquid. There is, of course, a considerable spread in the angular probability distributions, but there is strong preference for the alignment described. Figure 5 shows some of the evidence for the ring alignment for two different ionic liquids. In this figure, the z axis is centered at the midpoint of the surface with the vapor phase to the right (positive z). The rings in the top layer of the liquid just below the surface (from $z = -2$ to 0) show positive values of the P_2 function, demonstrating the NN axis in the ring tends to align parallel to the surface normal in this region. In contrast, the rather few molecules on the outside of the surface (positive z) lie flat on the surface and have negative values of P_2. Figure 6 shows how the butyl groups in [C_4mim][PF_6] stretch out into the vacuum. One can see from this figure how the densities of successive carbon atoms in the butyl side chain have maxima further and further toward the vacuum, while the most probable position

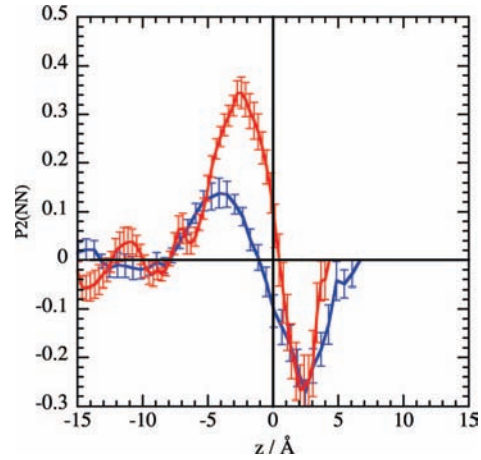

FIGURE 5. Cation orientational correlations near the interface. The averages $\langle P_2(\cos(\theta))\rangle$ for the angle between the NN direction in the ring and the surface normal are shown for [dmim][Cl] (red) and [C_4mim][Cl] (blue). These graphs demonstrate that the cations just below the surface are preferentially oriented with the NN axis vertical and the plane of the ring perpendicular to the plane of the surface.

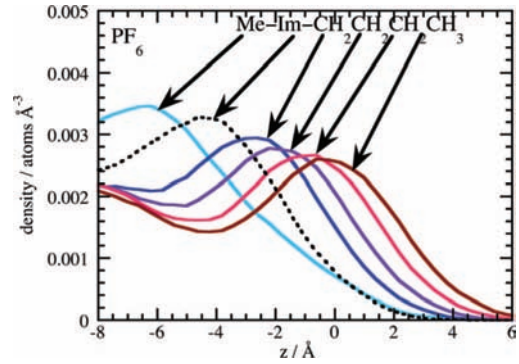

FIGURE 6. Density distributions for the carbon atoms in the butyl side chain, the methyl group, and the ring center. This shows that the butyl side chains extend into the vacuum and the methyl group points into the liquid. This figure was reproduced from ref 20, copyright 2006, with permission from the PCCP Owner Societies.

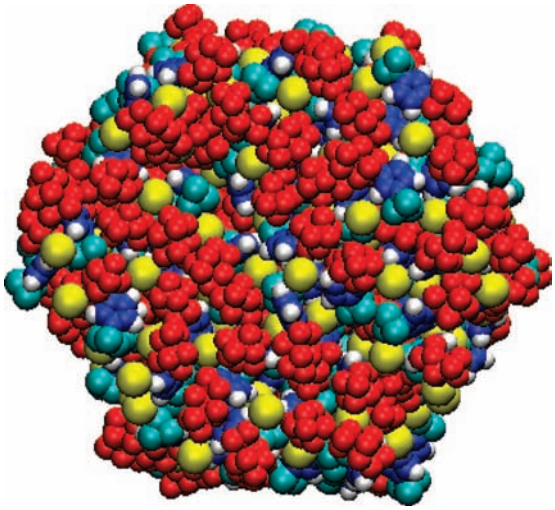

FIGURE 7. View looking down on the surface of [C_4mim][Cl]. The red butyl groups point toward the viewer, and the yellow chloride ions and some blue rings can be seen between them.

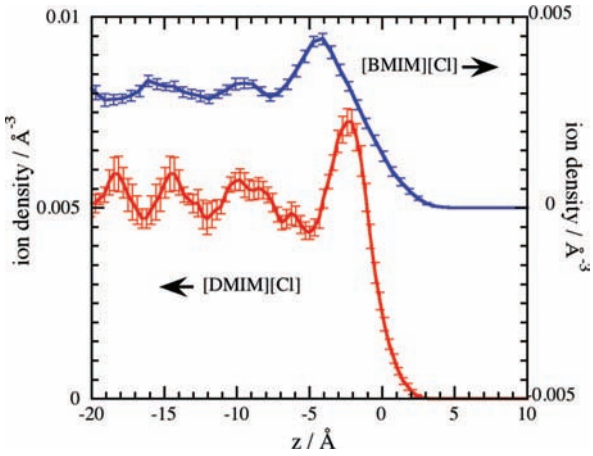

FIGURE 8. Densities of rings through surfaces of [C_4mim][Cl] (blue) and [dmim][Cl] (red). Note the region of enhanced ring density below the surface.

of the methyl carbon is, on average, nearer the liquid than the ring center. However, the butyl groups do not cover the surface, as can be seen from Figure 7, which shows a snapshot of the surfaces of [C_4mim][Cl]. The yellow chloride ions, which lie in the plane of the rings, can clearly be seen between the red butyl groups. The region of preferred cation alignment is also a region where the density of rings is a maximum and, indeed, the overall number density is higher than in bulk. This can be seen in Figure 8 and has been verified by X-ray reflection experiments.[21]

The anions are found to lie in the same plane as the rings of the cation, so that there is no segregation of cations and anions at the surface in this model. Any such segregation would give rise to a large surface dipole and a change in the electrostatic potential through the surface analogous to a liquid junction potential or to the work function of a metal. Although the liquid–gas surface potential is very difficult to measure experimentally, it is

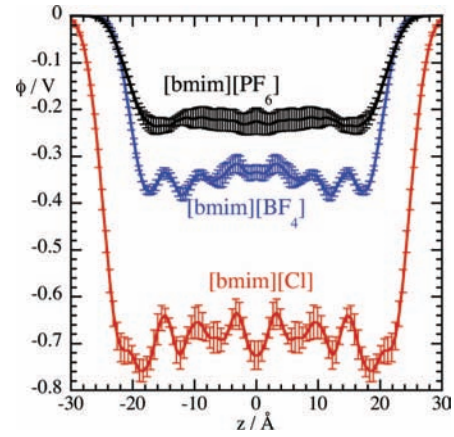

FIGURE 9. Variation of the electrostatic potential across liquid slabs of three ionic liquids. Note that in this and subsequent figures the z coordinate is centered at the center of the liquid slab. This figure was reproduced from ref 20, copyright 2006, with permission from the PCCP Owner Societies.

readily accessible in a simulation. Integrating Poisson's equation along the direction of the surface normal, one obtains

$$\varphi(z_0) - \varphi(-\infty) = (\varepsilon_0)^{-1} \int_{-\infty}^{z_0} (z - z_0)\rho(z)\mathrm{d}z \qquad (1)$$

where $\rho(z)$ is the average charge density at position z along the surface normal. Figure 9 shows the variation of potential through the surfaces of a number of [C_4mim] ionic liquids. The electrostatic potential is lower in the liquid than in the gas phase and the potential drop decreases as the size of the anion increases.

5. Confined Liquids

One of the applications of ionic liquids is in the construction of dye-sensitized solar cells.[22,23] These are photovoltaic devices consisting of a layer of nanoporous TiO_2, coated with a light-sensitive dye, clamped between two metallic electrodes. The interstices left between the TiO_2 grains are filled with a liquid electrolyte that dissolves a redox couple (usually I^-/I_3^-). A surprising feature of the cells is that, despite the high viscosity of the molten salt, the screening of the charge injected into the TiO_2 nanoparticles is achieved in less than 1 ps. We undertook simulations of a simple ionic liquid in nanoscale pores to elucidate this apparent anomaly. Our model consisted of [dmim][Cl] confined to slits about 2.5–4.5 nm wide, and we studied the liquid both in the absence of an applied field[24] and with an applied field.[25]

Even in the absence of an applied field, the structure of the liquid is affected by the presence of the solid–liquid interface. Figure 10 shows that there is a high density of ions next to the surface and that this induces density oscillations within the liquid. These density oscillations extend to a considerable depth, and even in the widest slit studied (4.5 nm), the liquid at the center of the slit is affected by the walls. Figure 11 shows that, just as at the gas–liquid interface, the cations are aligned near the interface. The cations that are nearest the wall lie flat against the wall, as is shown by the positive values of

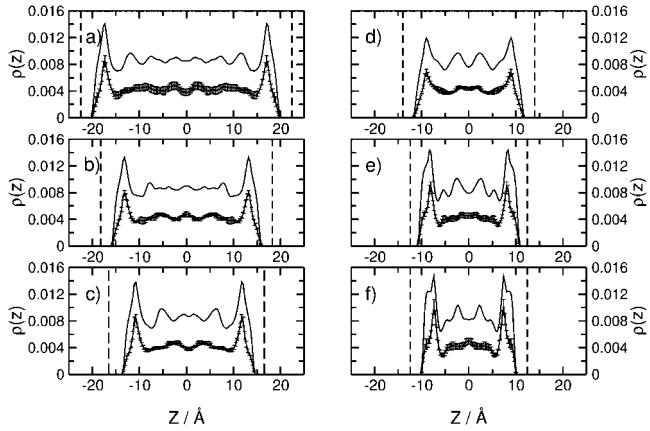

FIGURE 10. Lines with error bars represent the cation density calculated from the position of the center of the rings. Lines without error bars correspond to the sum of cation and anion densities. $\rho(z)$ is in angstroms. The interwall distances are (a) 44.9, (b) 36.5, (c) 33.0, (d) 28.0, (e) 26.4, and (f) 24.9 Å. The dashed vertical lines show the position of the walls. This figure was reproduced from ref 24, copyright 2005, with permission from the American Chemical Society.

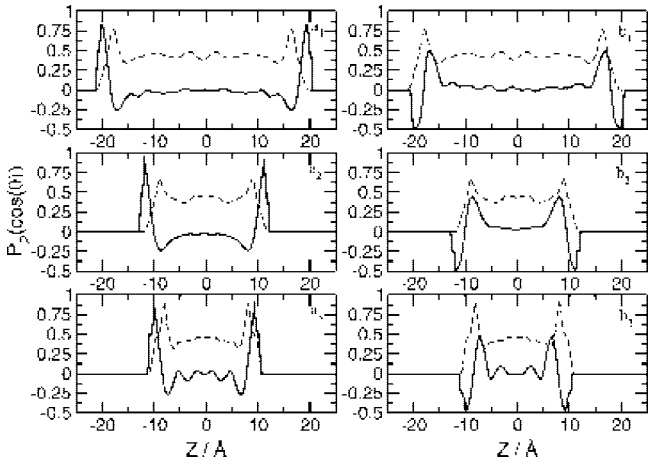

FIGURE 11. Orientational order parameter $P_2(\cos(\theta))$ along the confinement axis (continuous lines). The dashed lines are scaled cation density profiles. Plots a1, a2, and a3 show the orientation of an axis perpendicular to the cation plane as a function of the interwall distance: (a1) 44.9, (a2) 28.0, and (a3) 24.9 Å. Plots b1, b2, and b3 give the orientation of the NN vector connecting the two nitrogen atoms at the corresponding gap widths. This figure was reproduced from ref 24, copyright 2005, with permission from the American Chemical Society.

$P_2(\cos\theta_\perp)$ and negative values of $P_2(\cos\theta_{NN})$ next to the wall. However, the number of flat molecules is very small, and the bulk of the cations in the region of maximum density near the wall are tilted, with their rings and NN axes tending to be perpendicular to the wall. This is shown by a reversal of sign of the orientational order parameters as one goes away from the wall into the region of maximum density.

When the field is applied and the ions are allowed to equilibrate, one finds small changes in the ion distribution, which are shown in Figure 12. The most obvious change is a displacement of chloride ions toward the positively charged wall. Although there are only small changes in the positions of the ions and even less change

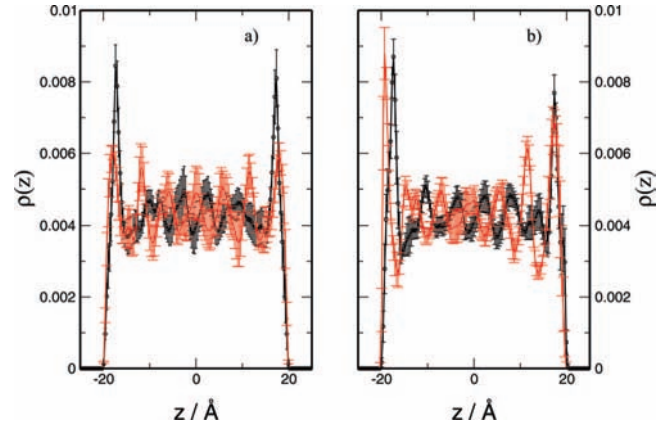

FIGURE 12. Ion number density profiles for [dmim] cations (black line) and chloride anions (red line) confined between two parallel walls, separated by 44.9 Å. Plots a and b correspond to the system without and with an external electric field generated by a uniform surface charge density, σ, of 2.0 μC/cm^2, respectively. The left wall has a positive charge. This figure was reproduced from ref 25, copyright 2007, with permission from the American Chemical Society.

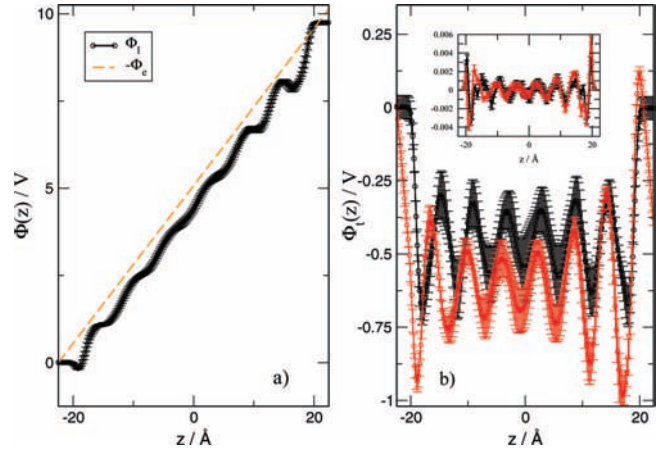

FIGURE 13. Electrostatic potential profiles (in volts) along the confinement axis (z). In a, the orange dashed line is minus the external electrostatic potential, while the bold line is the potential as a result of the liquid. In b, the red line depicts the resulting potential across the liquid slab. The black line corresponds to the electrostatic potential for a system without an external field. The inset of b shows the charge densities for the system with (red line) and without (black line) an external field. This figure was reproduced from ref 25, copyright 2007, with permission from the American Chemical Society.

in the cation orientation, the ion displacements are sufficient to screen most of the applied electric field. If the total potential drop across an empty 4 nm cell is 10 V, when filled with [dmim][Cl], it drops to 0.35 V. This is shown in Figure 13, where on the left are plotted minus the external potential and the liquid potential. It can be seen that they nearly cancel. The difference of these two curves gives the total potential, which is shown by the red line in the righthand part of the figure. The black line shows the corresponding potential in the absence of the applied field, which shows that there is a potential drop at the interface with an uncharged wall. This is similar to

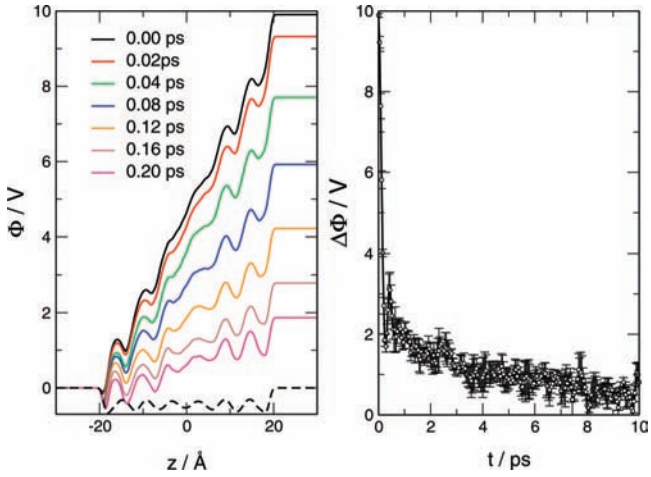

FIGURE 14. Electrostatic potential relaxation. (a) Electrostatic potential profile along the confinement axis for different times after the electric field was switched off ($t = 0$ ps). (b) Electrostatic potential difference ($\Delta\Phi$) between the two electrodes as a function of time (with error bars). This figure was reproduced from ref 25, copyright 2007, with permission from the American Chemical Society.

that seen in the liquid slabs (Figure 9). In the presence of the electric field, the potential distribution is distorted. As mentioned before, in slits of this size (4 nm), bulk behavior is not attained at the center. If it were, there would be a region of constant potential. The influence of the wall on the potential as well as on the structure extends for more than 2 nm.

As we have mentioned earlier, the screening of the field is important to the action of a dye-sensitized solar cell, and experimentally, it is found to occur on a picosecond time scale. Figure 14 shows the decay of the screening potential when the field is turned off. It can be seen that the relaxation process is characterized by two regimes: a fast process, occurring in less than 0.2 ps, that accounts for 80% of the screening, and a second slower process, with a decay time of 8 ps. Both of these times are fast compared to macroscopic diffusion times, which is not unexpected, because we have seen that the screening is accomplished by small displacements of ions.

6. Concluding Remarks

Although it is less than 10 years since the first simulations of room-temperature ionic liquids have been carried out, it is already apparent that such simulations have given much insight into the molecular basis of properties of these interesting and important liquids. Because it is impractical to perform long and large simulations with ab initio methods, classical force fields are essential. One question is how sensitive the results are to the parametrization. Many properties should be described by all force fields, which contain the essential physics, namely, the charges and shapes of the ions. Other properties, in particular, exact values of dynamical constants, such as diffusion, or accurate thermodynamic properties, such as solubilities, are likely to be more sensitive to the type of force field and parameters used. However, trends are well-described by simple classical models, even when the ring is treated as a rigid unit. We have found that we can describe the local structure of the liquid around solutes and at interfaces well and have demonstrated the molecular basis for aspects of solubility and behavior at interfaces.

We are grateful to the Engineering and Physical Sciences Research Council (EPSRC) for financial support of this work over the last 10 years (GR/S41562 and EP/D029538/1) and to the members of the QUILL laboratory for many discussions and suggestions. J.B.H. thanks the University of New South Wales (UNSW) for ongoing financial support.

References

(1) Allen, M. P.; Tildesley, D. J. *Simulation of Molecular Liquids*; Oxford University Press: New York, 1987.
(2) Hanke, C. G.; Price, S. L.; Lynden-Bell, R. M. Intermolecular potentials for simulations of liquid imidazolium salts. *Mol. Phys.* **2001**, *99*, 801–809.
(3) de Andrade, J.; Boes, E. S.; Stassen, H. A force field for liquid state simulations on room temperature molten salts: 1-Ethyl-3-methylimidazolium tetrachloroaluminate. *J. Phys. Chem. B* **2002**, *106*, 3546–3548.
(4) Anthony, J. L.; Maginn, E. J.; Brennecke, J. F. Solubilities and thermodynamic properties of gases in the ionic liquid 1-*n*-butyl-3-methylimidazolium hexafluorophosphate. *J. Phys. Chem. B* **2002**, *106*, 7315–7320.
(5) Margulis, C. J.; Stern, H. A.; Berne, B. J. Computer simulation of a "green chemistry" room-temperature ionic solvent. *J. Phys. Chem. B* **2002**, *106*, 12017–12021.
(6) Chaumont, A.; Wipff, G. Solvation of M^{3+} lanthanide cations in room-temperature ionic liquids. A molecular dynamics investigation. *Phys. Chem. Chem. Phys.* **2003**, *5*, 3481–3488.
(7) Shim, Y.; Duan, J. S.; Choi, M. Y.; Kim, H. J. Solvation in molecular ionic liquids. *J. Chem. Phys.* **2003**, *119*, 6411–6414.
(8) Canongia Lopes, J. N.; Deschamps, J.; Padua, A. A. H. Modeling ionic liquids using a systematic all-atom force field. *J. Phys. Chem. B.* **2004**, *108*, 2038–2047.
(9) Yan, T.; Burnham, C. J.; Del Pópolo, M. G.; Voth, G. A. Molecular dynamics simulation of ionic liquids: The effect of electronic polarizability. *J. Phys. Chem. B* **2004**, *108*, 11877–11881.
(10) Yan, T.; Li, S.; Jiang, W.; Gao, X.; Xiang, B.; Voth, G. A. Structure of the liquid–vacuum interface of room-temperature ionic liquids: A molecular dynamics study. *J. Phys. Chem. B* **2006**, *110*, 1800–1806.
(11) Resende Prado, C. E.; Del Pópolo, M. G.; Youngs, T. G. A.; Kohanoff, J.; Lynden-Bell, R. M. Molecular electrostatic properties of ions in an ionic liquid. *Mol. Phys.* **2006**, *104*, 2477–2483.
(12) Youngs, T. G. A.; Del Pópolo, M. G.; Kohanoff, J. Development of complex classical force fields through force matching to ab initio data: Application to a room-temperature ionic liquid. *J. Phys. Chem. B* **2006**, *110*, 5697–5707.
(13) Lynden-Bell, R. M.; Youngs, T. G. A. Using DL_POLY to study the sensitivity of liquid structure to potential parameters. *Mol. Simul.* **2006**, *32*, 1025–1033.
(14) Hanke, C. G.; Johansson, A.; Harper, J. B.; Lynden-Bell, R. M. Why are aromatic compounds more soluble than aliphatic compounds in dimethylimidazolium ionic liquids? A simulation study. *Chem. Phys. Lett.* **2003**, *374*, 85–90.
(15) Harper, J. B.; Lynden-Bell, R. M. Macroscopic and microscopic properties of aromatic compounds in ionic liquids. *Mol. Phys.* **2004**, *102*, 85–94.
(16) Lynden-Bell, R. M.; Atamas, N. A.; Vasilyuk, A.; Hanke, C. G. Chemical potentials of water and organic solutes in imidazolium ionic liquids: A simulation study. *Mol. Phys.* **2002**, *100*, 3225–3229.
(17) Hanke, C. G.; Atamas, N.; and Lynden-Bell, R. M. Solvation of small molecules in imidazolium ionic liquids: A simulation study. *Green Chem.* **2002**, *4*, 107–111.
(18) Lynden-Bell, R. M. Gas–liquid interfaces of room temperature ionic liquids. *Mol. Phys.* **2003**, *101*, 2625–2633.
(19) Lynden-Bell, R. M.; Kohanoff, J.; Del Pópolo, M. G. Simulation of interfaces between room temperature ionic liquids and other liquids. *Faraday Discuss.* **2005**, *129*, 57–67.

(20) Lynden-Bell, R. M.; Del Pópolo, M. G. Simulation of the surface structure of butylmethylimidazolium ionic liquids. *Phys. Chem. Chem. Phys.* **2006**, *8*, 949–954.
(21) Sloutskin, E.; Lynden-Bell, R. M.; Balasubramanian, S.; Deutsch, M. The surface structure of ionic liquids: Comparing simulations with X-ray measurements. *J. Chem. Phys.* **2006**, 125, article number 174715.
(22) Grätzel, M. Applied physics—Solar cells to dye for. *Nature* **2003**, *421*, 586–587.
(23) O'Regan, B.; Grätzel, M. A low-cost, high efficiency solar-cell based on dye-sensitized colloidal TiO_2 films. *Nature* **1991**, *353*, 737–740.
(24) Pinilla, C.; Del Pópolo, M. G.; Lynden-Bell, R. M.; Kohanoff, J. Structure and dynamics of a confined ionic liquid—Topics of relevance to dye sensitized solar cells. *J. Phys. Chem. B* **2005**, *109*, 17922–17927.
(25) Pinilla, C.; Del Pópolo, M. G.; Kohanoff, J.; Lynden-Bell, R. M. Polarization relaxation in an ionic liquid confined between electrified walls. *J. Phys. Chem. B* **2007**, *101*, 4877–4884.
(26) Del Pópolo, M. G.; Lynden-Bell, R. M.; Kohanoff, J. Ab initio simulation of a room temperature ionic liquid. *J. Phys. Chem. B* **2005**, *109*, 5895–5902.

AR700065S